Research Square

Preprints are preliminary reports that have not undergone peer review.
They should not be considered conclusive, used to inform clinical practice,
or referenced by the media as validated information.

Preparation of corrosion resistant and anti-ultraviolet radiation anti-reflection film with IBTS and TEOS

Beiping Dong
Mingxuan Li
Zhaorui Li
Zhihang Shang
Xiang Zhou
Lifang Nie
nielifang@tiangong.edu.cn

Juncheng Liu

Research Article

Keywords: IBTS, Anti-reflection, Anti ultraviolet radiation, Thin film, Solar cell

Posted Date: April 3rd, 2025

DOI: https://doi.org/10.21203/rs.3.rs-6242216/v1

License: This work is licensed under a Creative Commons Attribution 4.0 International License.
Read Full License

Additional Declarations: No competing interests reported.

Version of Record: A version of this preprint was published at Journal of Sol-Gel Science and Technology on August 29th, 2025. See the published version at https://doi.org/10.1007/s10971-025-06841-2.

Preparation of corrosion resistant and anti- ultraviolet radiation anti-reflection film with IBTS and TEOS

Beiping Dong, Mingxuan Li, Zhaorui Li, Zhihang Shang, Xiang Zhou, Lifang Nie*, Juncheng Liu*

School of Materials Science and Engineering, Tiangong University, Tianjin 300387, China.

* Corresponding author: nielifang@tiangong.edu.cn (Dr. Nie); jchliu@tiangong.edu.cn (Prof. Liu)

Abstract: The anti-reflective film is one of the important and economical ways to improve the photoelectric conversion efficiency of solar cells. In order to improve the weather ability of SiO_2 antireflection film prepared with sol-gel method, the mixture of isobutyl triethoxysilane (IBTS) and tetraethyl silicate (TEOS) as silicon source was used to prepare the porous anti-reflection film with dip-coating, in which polyethylene glycol mono-methyl ether (mPEG) as porogen. The effects of the addition amount of IBTS on the structure and properties of the anti-reflection film were investigated. The results show that both the porosity and the transmittance of the film increased first and then decreased with the increase of the amount of IBTS. When the amount of IBTS was 6 ml, the film's average transmittance within 380-1100 nm wavelength range reached the maximum 93.61%, 4.4 percentage points higher than that of the glass substrate. Moreover, the film's adhesion strength reached grade 0, and its hardness was greater than 9 H. When the coated glass was used as the cover instead of the substrate glass, the efficiency of monocrystalline silicon solar cells improved from 11.64% to 12.26%, a relative increase of 4.93%. The film's hardness and adhesion strength changed little after 100 hours of UV lamp irradiation, while the average transmittance in the range of 380-1100 nm decreased with 0.45 percentage points. After immersion in hydrochloric acid solution for 80 h, the film hardness decreased to 8H, and the adhesion strength decreased to grade 1, while the transmittance increased with the increase of immersion time. When the immersion time reached 100 h, the film's transmittance increased 0.81%.

Keywords: IBTS; Anti-reflection; Anti ultraviolet radiation; Thin film; Solar cell

1 Introduction

Commercial solar cells generally have glass covers to prevent damage and delay the attenuation of photoelectric conversion efficiency [1]. The efficiency of solar cells can be effectively improved

with anti-reflection film deposited on the glass cover surface. Silicon based solar cells require glass covers with high transmittance within the 380-1100 nm spectral range. The single layer anti-reflection film can be widely used in solar cells due to its simple process and low cost. Its refractive index must be lower than that of the cover glass (refractive index is 1.52) [2].

Generally, the refractive index of fluoride among the dense materials is low. For example, the refractive index of MgF_2 is 1.38 [3] and that of CaF_2 is 1.44 [4], which are lower than that of photovoltaic glass n_0. Although their film can effectively improve the light transmittance of the glass cover, the anti- reflection effect is not ideal, because their refractive index is still much larger than the ideal refractive index$\sqrt{n_0}$, about 1.23.

The refractive index of composite film is determined with the refractive indices of various materials in the film. The porous film can be regarded as a heterogeneous film composed of air and film materials. The refractive index of air is 1.0 [5], which is the lowest in nature. The higher the porosity of the porous film, the lower the refractive index. The sol-gel method is often used to prepare anti-reflection film on glass substrates in combination with dip-coating spraying, spinning, etc. It is not only simple and cheap, but also easy to adjust the porosity of the film [6]. Wang [7] et al. prepared porous single-layer SiO_2 film with sol-gel method, of which average transmittance within 380-1100 nm band increased 4.54 percentage points. Yuan [8] et al. prepared monolayer porous SiO_2/poly-methyl-hydro-siloxane (PMHS) composite anti-reflection film with sol-gel method, which improved the transmittance of soda lime glass at 400-800 nm 7 percentage points. Chi [9] et al. used ammonia to treat the surface of the anti-reflection film prepared with the sol-gel method, of which refractive index was adjusted via the ammonia treatment time changing. The treated SiO_2 anti-reflection film finally achieved an average transmittance of 98% in the 350-1400 nm band. Unfortunately, these works rarely involved the mechanical properties or UV radiation resistance of thin film.

Solar cells are usually used in many places with harsh environments, such as deserts, mountains, plateaus, etc. Therefore, solar cells generally need glass cover protection to reduce the impact of harsh environment, and the anti-reflection film applied to glass cover will directly face harsh environment. Therefore, in order to reduce light loss and improve the power generation efficiency of solar cells through anti-reflection film, the weather fastness of anti-reflection film (including resistance to ultraviolet radiation, acid rain erosion, wind and sand abrasion, etc.) is a problem that cannot be ignored [10, 11].

The ultraviolet radiation can catalyze the oxidation reaction of substances, leading to the aging of substances [12]. Because the ultraviolet light is easy to irradiate into the interior of the anti-reflection film with large aperture, the ultraviolet aging resistance is an important performance index of the porous anti-reflection film. SiO_2 anti-reflection film prepared with sol-gel method is usually synthesized with organic compounds [13], which are very sensitive to the aging effect of ultraviolet ray. After the anti-reflection film is aged with ultraviolet light in the sun, it will no longer have the original optical and mechanical properties, resulting in the anti-reflection film no longer having good anti-reflection effect, or even hindering the transmission of sunlight.

Although the porous film has obvious advantages on anti-reflection performance, the pore size of the porous structure on its surface is too large, the capillarity phenomenon is easy to occur, causing water to enter [14]. The water can carry harmful substances to the interface between the anti-reflection film and the substrate through the pores of the anti-reflection film, damaging the combination of the anti-reflection film and the substrate, and can also corrode the structure of the anti-reflection film. Since the refractive index of water is 1.33, when water exists in the pores, the refractive index of the film will increase, and its anti-reflection effect will reduce. Du [15] et al. prepared porous para boric sulfuric acid anodic oxide film (BSAA) with the anodic oxidation technology. They improved its corrosion resistance with boric acid. It was found that the pore diameter gradually decreased and the corrosion resistance increased with the increase of boric acid content from 0 to 8 g/L. However, when it exceeded 8g/L, the effect of corrosion resistance gradually decreased. Li et al. [16] used ammonium fluotitanate to seal the surface on the anodized film, and modified it with perfluorooctanoic acid, which can effectively block the corrosion medium and inhibit the development of corrosion., Garcia-Cabezon [17] proposed a strategy for the corrosion protection of porous materials with conductive polymers and nanocomposites of polymers and nanoparticles. TiO_2 porous film were modified the corrosion protection with pyrrole, aniline, 3,4-ethylenedioxythiophene, poly (phenylene sulfonate), and sodium dodecylbenzene sulfonate (DBSA).

Due to its small molecular structure, isobutyl triethoxysilane (IBTS) can penetrate the cementitious surface, penetrate into the film, react with the water molecules in the film and substrate, form a permanent and firm waterproof layer, and inhibit water absorption. IBTS is a commonly used anti-corrosion agent in the concrete industry, which is widely used in the anti-corrosion protection of large projects, such as roads, bridges, tunnels and docks. Yu [14] et al. studied the water-resistant principle of the material surface after the material surface was coated with IBTS, and proposed that

IBTS blocked the ion transport channels through iBu-Si-O-Si, playing a role in the corrosion prevention. Li [18] et al. used TEOS and IBTS as raw materials to prepare a composite film with sol-gel method, which could effectively inhibit chloride ion corrosion. Geng [19] and others modified the composite silane film (TEOS and IBTS) with graphene oxide (GO), further improved the corrosion resistance of the composite silane film. In addition, IBTS can resist UV aging due to its special molecular structure.

In order to improve the weather fastness of the porous anti-reflection film, IBTS as the silane blended with TEOS, and used the sol-gel method to prepare SiO_2 film. The effects of the addition amount of IBTS on the microstructure, optical properties and mechanical properties of the film were studied, and the resistance to hydrochloric acid corrosion and ultraviolet radiation was tested.

2 material and experiment

2.1 Sample preparation

Sol preparation: Dissolve 10 ml of tetraethyl silicate (TEOS,>99%, Shanghai Aladdin Biochemical Technology Co., Ltd.) and various volumes of isobutyl triethoxysilane (IBTS,>98%, Shanghai Aladdin Biochemical Technology Co., Ltd.) in 100 ml of ethanol (EtOH,>99.7%, Tianjin Fengchuan Chemical Reagent Technology Co., Ltd..The volume of isobutyl triethoxysilane was 2 ml, 4 ml, 6 ml, 8 ml, 10 ml, corresponding to the volume ratio to TEOS of 0,0.2, 0.4, 0.6, 0.8, 1.Mixing evenly, add hydrochloric acid (HCl, 36 wt.%, Tianjin Fengchuan Chemical Reagent Technology Co., Ltd.) and deionized water to keep stirring for 2h. Then the mixed solutions were moved into a conical flask andreflowed at 60 ℃ for another 2h. Add 0.6 g of polyethylene glycol monomethyl ether (mPEG 1900) and stir until completely dissolved. After aging for 5 days, the prepared transparent sols can be used for dip-coating.

Film preparation: In this experiment, photovoltaic white glass (89.2% visible light transmittance) was used as the substrate, and size was 50 ×20 × 2 mm^3。Soapy water, ethanol, acetone and distilled water was used to ultrasonic clean for 30 min in turn, and then the cleaned substrate was baked at 80℃ until completely dried. Dipping lifting method (the model of the lifting machine is SYDC-100) was used for film preparation. The lifting speed is 800 *um*/s and the number of lifting is 1. After dip coating, the gel film was formed on the surface of the glass substrate after drying at 80 ℃ for 1h in the oven. Then the substrate was transferred to the muffle furnace to calcine at 400 ℃ for 1h to obtain porous SiO_2 film. For comparison, a proper amount of sol was dried and calcined with the film sample to obtain a powder sample, which was used to analyze the structure, chemical bond

and functional group information of thin film SiO_2 particles.

2.2 Test characterization

The crystalline of SiO_2 powder was analyzed with X-ray diffraction (XRD, D8 Discover, Bruker, Germany) and the chemical bonds and functional groups of SiO_2 powder were analyzed with Fourier transform infrared spectroscopy (FTIR, Nicolet iS50, Thermo Fisher Scientific, USA). Scanning electron microscopy (SEM, S4800, Hitachi, Japan) was used to observe the surface micromorphology of the synthesized SiO_2 films. The transmittance of the film at 380-1100 nm was measured with ultraviolet visible near-infrared spectrophotometer (UV Vis Nir, UH4150, Hitachi, Japan). The refractive index of the film was measured with a spectral ellipsometer (Syscos, China).

Use a pencil hardness tester (model: QHQ-A) to measure the hardness of the SiO_2 film (Chinese national standard GB/T1727-92 [20]). The hardness is expressed in accordance with the model of pencil across the film, and the model with the highest hardness is 9 H. When the pencil is scratched on the film, the included angle with the film is 45°. Adhesion is tested with tape pulling method. The specific method is to use a baige knife (model: QFH-SH600, in accordance with GB/T 1727-1992. [21]) to vertically cut a space of 1mm on the film surface, and then apply transparent tape on the film surface for 3 minutes. The angle between the end of the tape and the film surface should be kept at 90°, and then the tape is pulled down from the film surface at a certain speed. After 20 repetitions, measure the area of the damaged film to characterize the adhesive strength of the film. There are six levels of film adhesion, which gradually deteriorate from level 0 to level 5 [21].

After soaking in 0.5mol/L hydrochloric acid solution for 20, 40, 60, 80 and 100 hours, respectively, the film was washed with distilled water and moved into an oven at 80 ℃ for drying for 1 hour. The optical and mechanical properties were tested to characterize the corrosion resistance of the film. Illuminate the film with 250 W ultraviolet lamp in a 2.5 m^3 confined space to simulate ultraviolet radiation. The optical and mechanical properties of the films were compared before and after UV irradiation for 20, 40, 60, 80 and 100 h. Using the coated glass and blank substrate glass as the cover, the current density open circuit voltage (*Jsc-Voc*) curve and photoelectric conversion efficiency (*PCE*) of the monocrystalline silicon solar cell were measured by the solar cell test system (*CEL-IV*, Beijing China Education Au light Co., Ltd.).

3 Results and Discussion

The XRD spectrum of SiO_2 powder obtained is shown in Fig. 1. The sol without IBTS could not

be made into powder, so it is not characterized. JCPDS No. 05-0490 is a Standard PDF card of phase α-SiO_2 crystal powder, which is the most common crystalline phase of SiO_2 at a temperature far below 573 ℃ [22]. It can be seen that the XRD spectrum of each sample only had a wide diffraction peak between 15° and 35° , which was the so-called steamed bread peak, indicating that the prepared SiO_2 powder was amorphous [23, 24].

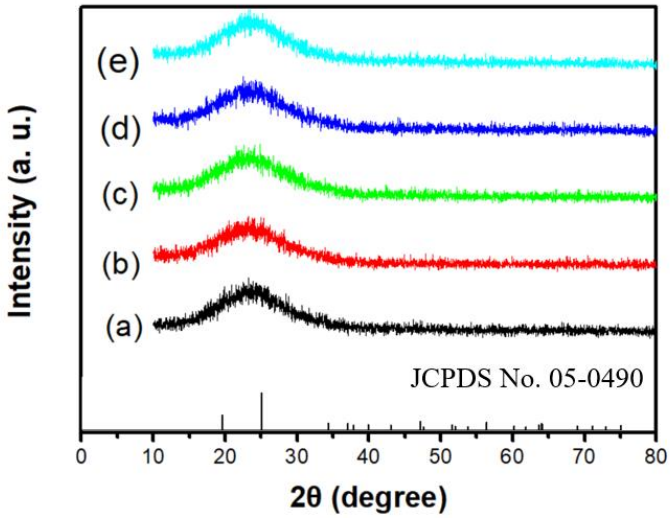


Fig. 1. XRD spectra of SiO_2 Powder Obtained with Sol Calcination with Different Volume Ratios: (a) 0.2； (b) 0.4； (c) 0.6； (d) 0.8； (e) 1.

Fig. 2 shows the effect of IBTS addition on the surface morphology of SiO_2 films. It can be seen that when IBTS is not added （Figure a), very fine SiO_2 particles were formed with an average particle size of ~10nm . This is because in the sol reaction process, no IBTS provides iBu Si OH and only Si - $(OH)_4$ in the group condenses with each other or with itself. This process is very slow, so the size of the SiO_2 particles obtained after calcination is small. In addition, there was no isobutyl on the surface of the condensation body to prevent the condensation process and the combination between each condensation body was very tight, thus a dense film was formed. When IBTS was added, the average particle size of SiO_2 increased to ~50 nm, which was shown in Fig(b)-Fig(f). When the ratio of IBTS to TEOS is 0.2, as shown in Fig. 2 (b), the particles were agglomerate with low porosity, but there were some fine cracks between each aggregate. When the ratio of IBTS to TEOS was 0.4, the cracks further expanded, and the porosity of the film was increased, as shown in Fig. 2 (c). When the ratio of IBTS to TEOS is 0.6, as shown in Figure 2 (d), the film was more porous and, the particle distribution was irregular. The gap between each particle was further enlarged. When the ratio of IBTS to TEOS is 0.8, as shown in Figure 2 (e), the particle distribution was gradually uniform and the porosity decreased along with the porosity of the geomembrane begins to decrease. When the ratio of IBTS to TEOS was1, the particle distribution is more uniform and denser, and the porosity is

further reduced, as shown in Fig. 2 (f).

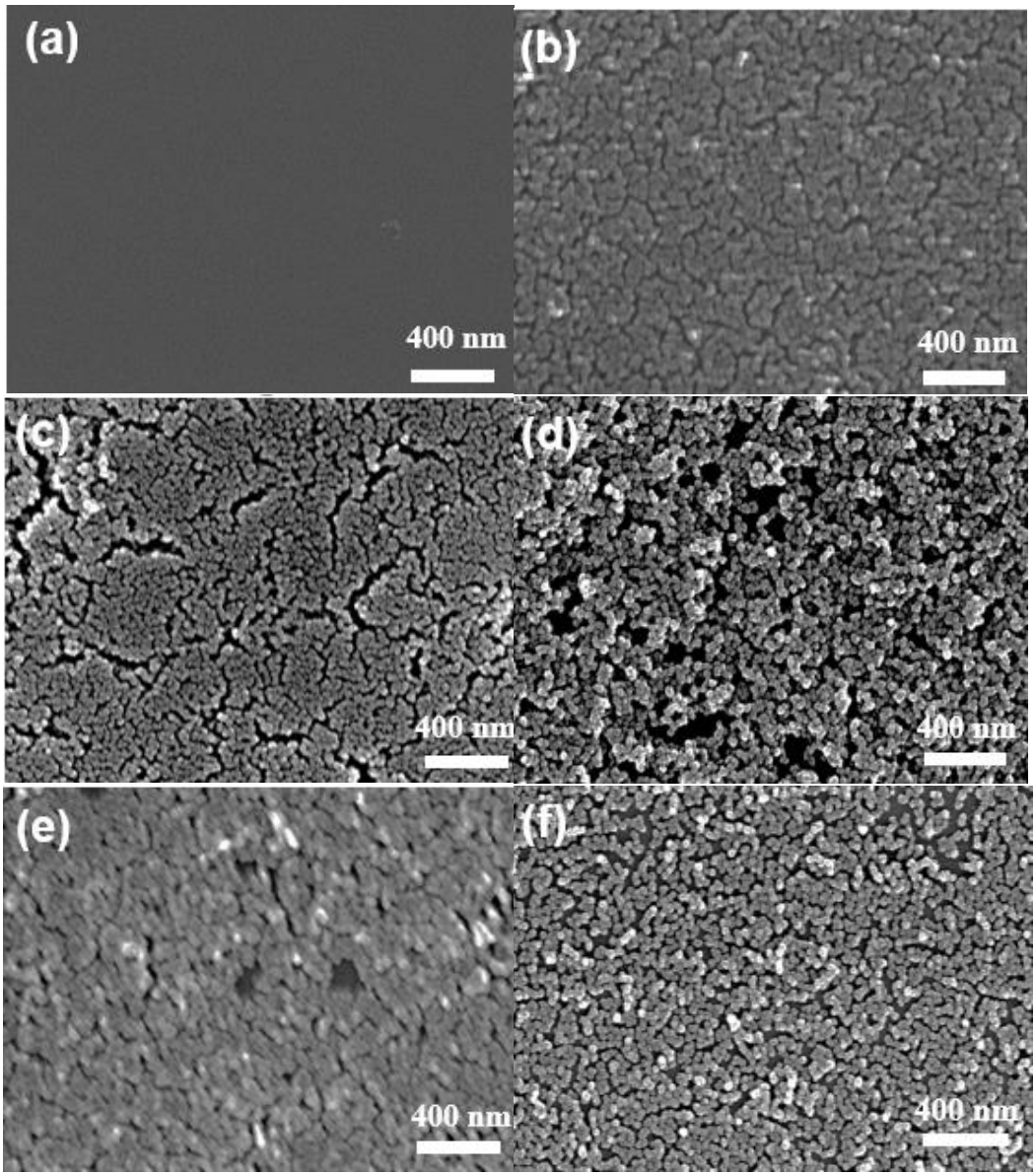


Fig. 2. Effect of IBTS addition on the surface morphology of anti-reflection film:
(a) without IBTS; (b) 2 ml； (c) 4 ml； (d) 6 ml； (e) 8 ml; (f)10 ml.

$Si(OH)_4$ obtained from hydrolysis of TEOS in the reaction system is condensed in three-dimensional space to form nano SiO_2 particles. The IBTS added is hydrolyzed to form iBu-Si -$(OH)_3$, which is condensed with the Si-OH on the surface of nano SiO_2 particles. The iBu Si group is connected to the surface of nano SiO_2 through Si-O-Si chemical bond. When the amount of IBTS is small, the iBu-Si formed with hydrolysis will all condense with $Si(OH)_4$ produced with TEOS, and the remaining $Si(OH)_4$ will condense with each other. The presence of iBu-Si will promote the formation of cracks between cluster particles, as shown in Fig. 2 (b) and (c). When the amount of iBu-Si is 6 ml, the amount of iBu Si is just grafted onto almost all $Si(OH)_4$ groups, the gap between particles increases, and even holes appear, as shown in Fig. 2 (d). Since then, with the increase of the

amount of IBTS addition, the concentration of iBu-Si-$(OH)_3$ generated in the solution is increased. Although it has been unable to fully branch with $Si(OH)_4$, iBu-Si-$(OH)_3$ itself will also undergo condensation, leading to the increase of particle concentration in the sol and the densification of the film, as shown in Fig. 2 (e) and (f).

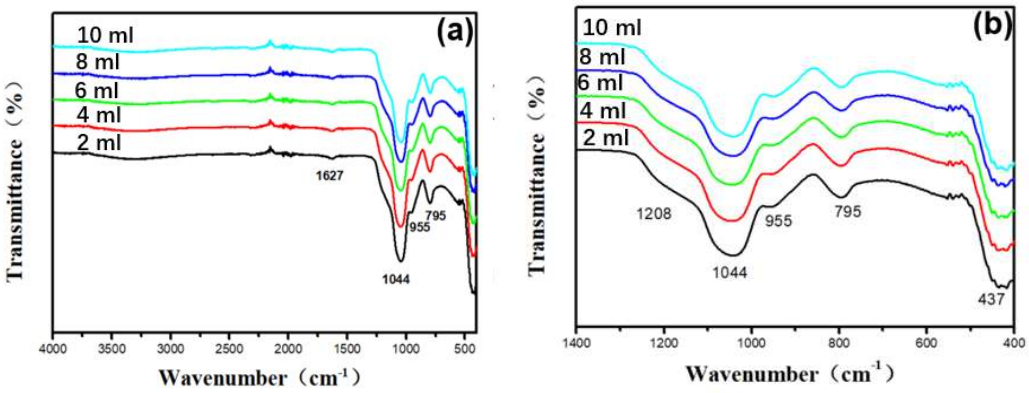


Fig.3. (a) Effect of IBTS addition on FTIR spectra of SiO_2 powders; (b) Partial enlarged detail.

The FTIR spectra (400-4000 cm^{-1}) of the powder obtained by calcining the SiO_2 gel at 400 ℃ is shown in Fig. 3 (a), and Fig. 3 (b) is a locally enlarged view. In Fig. 3 (b), the characteristic peak at 1044 cm^{-1} was the asymmetric tensile vibration of the three-dimensional Si-O-Si network, and the characteristic peak at 795 cm^{-1} was caused by the symmetric stretching vibration of Si-O-Si. In addition, the Si-O-Si bending stretching vibration was the peak at wave number 437 cm^{-1}. The shoulder at wave number 955 cm^{-1} was caused by the bending vibration of Si-OH group. As the surface siloxane group undergoes the dehydroxylation during heating, the peak was not obvious [25-28] and weakens to shoulder. The characteristic peak at 1208 cm^{-1} corresponds to the symmetric stretching vibration of Si-R.

It can be seen that the vibration of Si-R (1208cm^{-1}) gradually increased with the increase of IBTS, which is due to the fact that enough alkyl is added to the reaction system. The vibration of Si-O-Si characteristic peaks (1044 cm^{-1}, 795 cm^{-1}) were gradually strengthened, because the concentration of reactant IBTS increased and SiO_2 particles were generated. The vibration of Si-OH (955 cm^{-1}) decreased because more IBTS and Si-$(OH)_3$ condensed into Si-O-Si and water.

Fig. 4 (a) shows effect of the amount of IBTS addition on the refractive index spectra of SiO_2 film. It can be seen that the refractive index of each SiO_2 film increased with the increase of wavelength in the range of 380-1100 nm. The refractive index of the film decreased first and then increased with the increase of IBTS content. When the IBTS content was 6 ml, the refractive index of SiO_2 film was the lowest, 1.31 at 550 nm. The refractive index changed with the amount of IBTS

addition, corresponding to the change of the porosity of the film. The higher the porosity, the lower the refractive index. As mentioned earlier, the refractive index of porous film was determined with the refractive index of air and other materials. The refractive index of air is 1, which is lower than any other natural material. Therefore, when the proportion of air in the film is higher, the refractive index of the whole film will be lower, which is closer to the ideal refractive index 1.23 required for anti-reflection of photovoltaic glass cover.

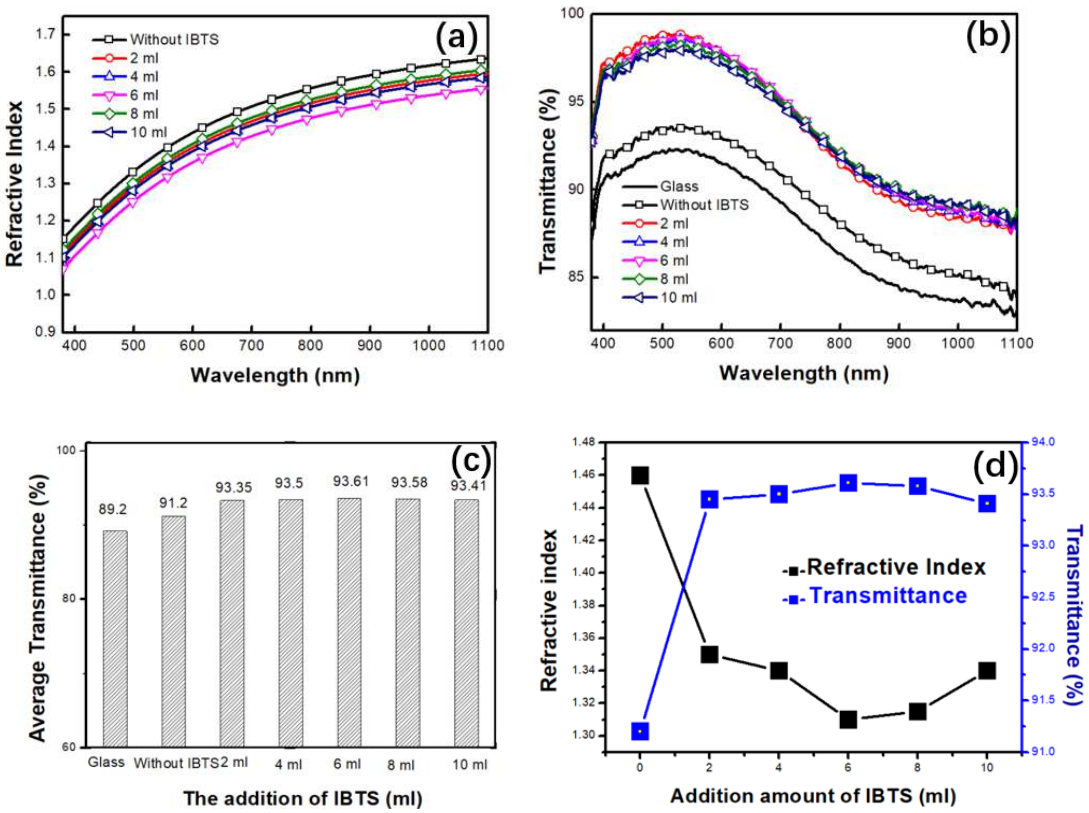


Fig.4. Effect of the IBTS addition on optical property of SiO_2 film：(a) the refractive index spectra; (b) the transmittance spectra; (c) the average transmittance; (d) the refractive index at 550nm and the average transmittance at 380-1100nm.

Figure 4 (b) shows the transmittance spectra of the film in the 380-1100 nm band. It can be seen that the shape of all spectral lines was similar, the transmissivity first increased and then decreased with the wavelength, and the highest transmissivity occurred at about 550 nm. Then, the transmissivity of all film (coated glass cover) was significantly higher than that of uncoated film, but the transmissivity of film without IBTS was not as high as that of film with IBTS.

Integrate the transmittance of the visible light area in the spectra of Fig. 4 (b) to obtain the average transmittance (380-1100 nm), as shown in Fig. 4 (c). In general, all SiO_2 film have good anti-reflection effect. It can be seen that the average transmittance of SiO_2 thin film increased first and then decreased with the increasing of IBTS addition. When the ratio of IBTS to TEOS was 0.6, the

average transmittance of the film was the highest in the wavelength range of 380-1100 nm, reaching 93.61%, which was 4.4 percentage points higher than that of the substrate. Fig. 4 (d) shows the influence of the amount of IBTS addition on the refractive index and transmissivity of the SiO_2 film at 550 nm. It can be seen that the refractive index of the film decreased from 1.34 to 1.31, and then increased to 1.35, while the change of the transmissivity was the opposite of the change in refractive index of the film .

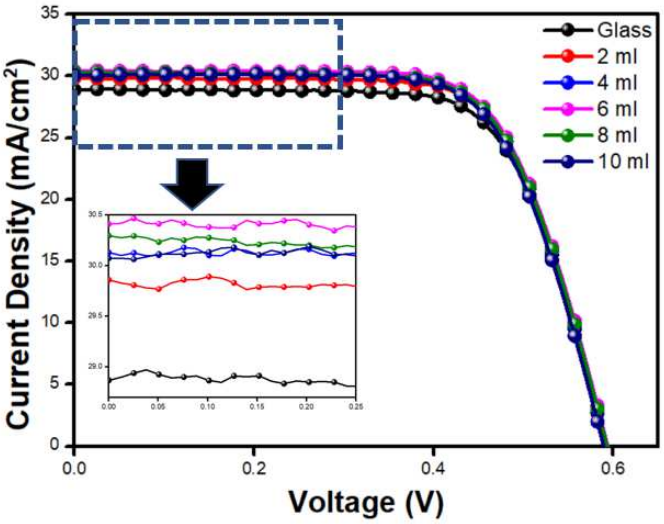


Fig.5. The *Jsc-V* curves of the monocrystalline silicon solar cell under the blank and the coated glass cover.

Figure 5 shows the current density voltage curve (*Jsc-V*) of the monocrystalline silicon solar cell under the blank glass cover and the coated glass cover. Obviously, the current density of solar cells with all coated glass covers was higher than that with blank glass covers. The results show that with the increase of IBTS content, the current density of monocrystalline silicon solar cells first increases and then decreases.

Table 1 lists the photovoltaic parameters of monocrystalline silicon solar cells covered under blank and coated glass cover. It can be seen that the open circuit voltage of 0.59 V remains stable, and the *Jsc* and *PCE* values first increase and then decrease with the addition content of IBTS. When the amount of IBTS added was 6 ml, the maximum of *Jsc* and *PCE* values was 30.41 mA/cm^2 and 12.56%, respectively. Comparing with the uncoated monocrystalline silicon solar cell, the *PCE* of the coated solar cell increased from 11.97% to 12.56%. That is, the absolute value of *PCE* increased with 0.59 percentage points, with a relative increase of 4.93%. The improvement of *Jsc* and *PCE* are attributed to the change of film transmissivity.

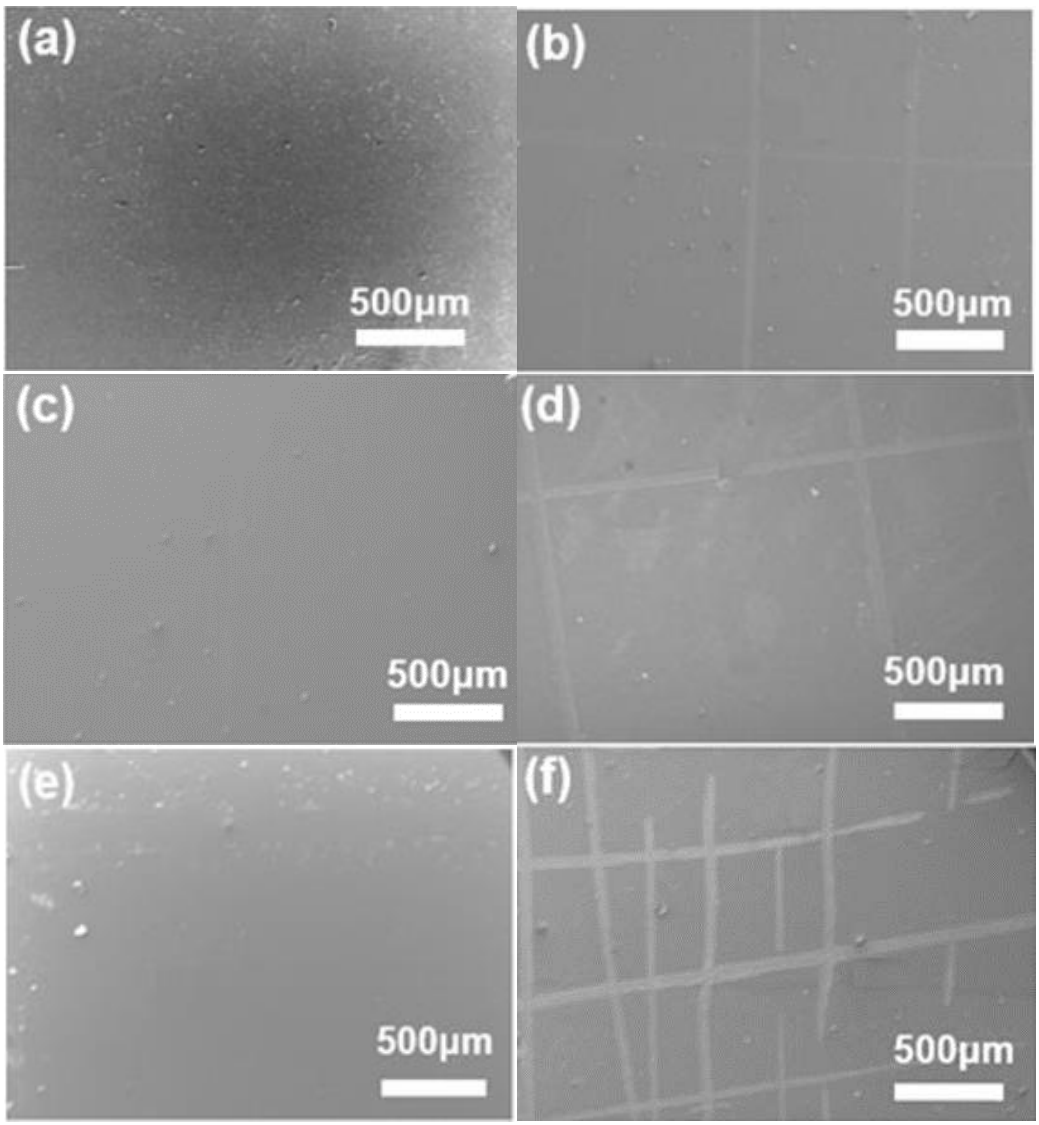


Fig. 6. Film Surface Morphology after Hardness Test with Pencil Method and Adhesion Test with Tape Tearing Method: (a), (b) are the SEM images after 9H pencil crossing without IBTS film and the SEM images after adhesion test respectively;(c), (d) SEM images of film with 6 ml IBTS after 9H pencil scratch and adhesion test scratch respectively; (e), (f) SEM images of film with 10 ml IBTS respectively after 9H pencil scratch and adhesion test scratch.

Fig. 6 shows the surface morphology of the film after hardness testing using the pencil method and adhesion testing using the tape tearing method. (a), (c), and (e) were scratch patterns on the 9 H pencil film, while (b), (d), and (f) were the surface morphology of the film after the tearing method. From Fig. 6 (a), (c), and (e), it can be seen that there were no clear and sharp scratches on the surface of all the films, indicating that the hardness of the films had reached 9H. From Fig. 6 (b), (d), and (f), it can be clearly seen that there was no significant detachment at the grid. According to the national standard [21], it can be judged that the adhesion of all SiO_2 films had reached level 0, which was the highest level. The high hardness is due to the use of hydrogen bonds in mPEG to bind particles with a high binding force. While the adhesion is due to the acid catalysis that caused the sol particles to combine positively with negatively charged hydroxyl groups on the glass surface, resulting in a high

binding force [29]. According to the FTRI spectra, there was a significant increase in Si-R active substances in the sol powder, indicating a stronger ability to bind to glass.

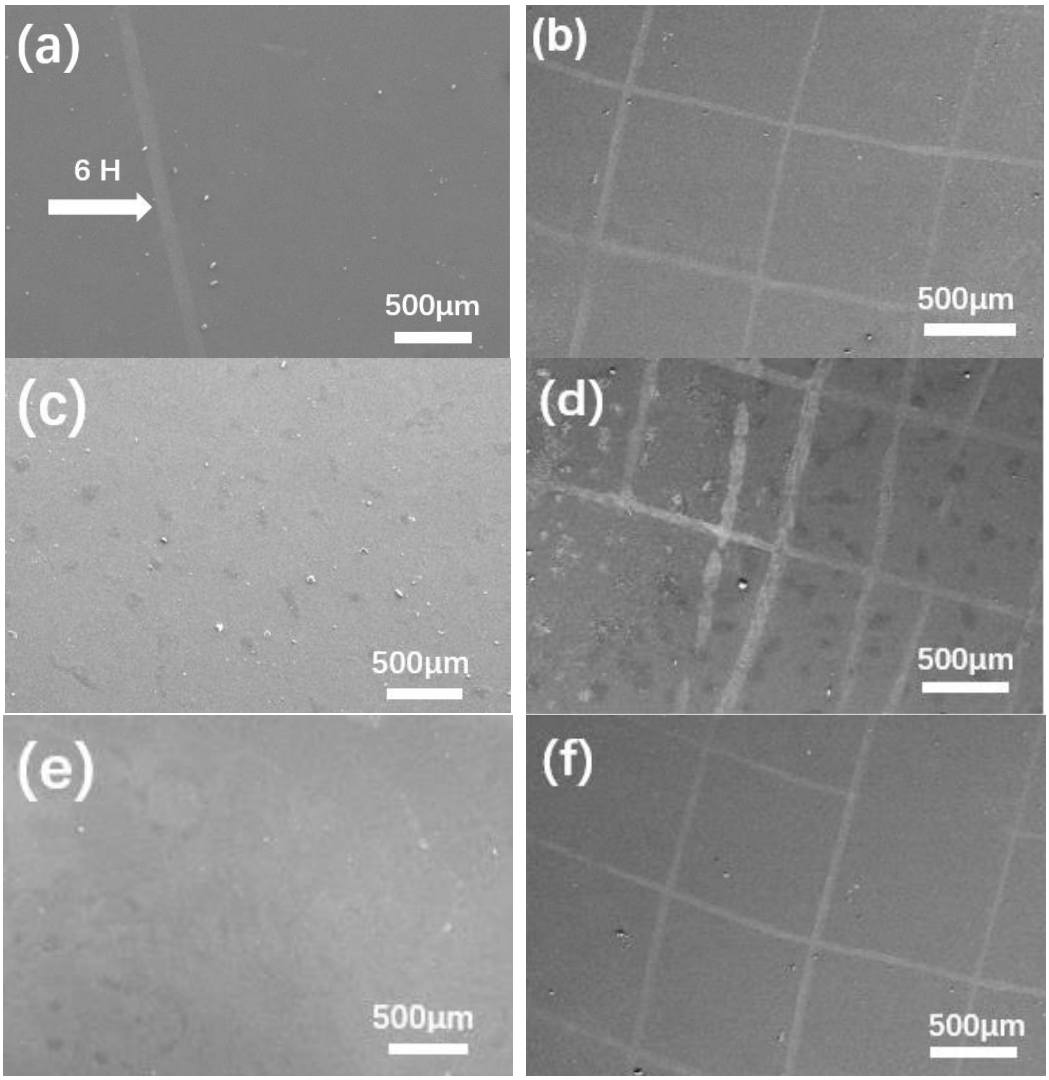


Fig. 7. Film Surface Morphology after Hardness Adhesion Test after Ultraviolet Irradiation: (a) And (b) are hardness scratch diagrams and adhesion scratch diagrams of film without IBTS after 60 h irradiation;(c) And (d) hardness scratch diagram and adhesion scratch diagram after irradiation of the film with 6 ml IBTS for 80 h;(e) And (f) hardness scratch diagram and adhesion scratch diagram after irradiation of 6 ml of IBTS film for 100 h.

Figure 7 is the SEM image of the film surface scratched by pencil and QFH after exposure to ultraviolet light. It can be seen from Fig. 7 (a) that the 6 H pencil had left a clear scratch on the film surface and the hardness could be judged as 5 H. Figure 7 (c) and (e) show that there was no obvious scratch on the film surface for 9 H pencil, which indicates that the hardness of SiO_2 film was still 9 H. According to Fig. 7 (b), (d) and (e), no obvious film peeling was observed at the scratch, indicating that the adhesion of the film was not significantly attenuated under ultraviolet light.

The reason for the decrease in hardness of the film without IBTS is that the particle size was small and the film-forming property was poor. Therefore, after exposing to ultraviolet radiation, the

connecting bonds between the outermost layer of particles of the film were damaged, and then caused the hardness to reduce. The film with IBTS had larger particle size and certain porosity and the bond perpendicular to the glass surface was not greatly affected. In addition, the SiO_2 film had small aperture. When the ultraviolet ray entered the film, it is easy to scatter because of its short wavelength, preventing the ultraviolet ray from penetrating into the anti-reflection film. It can protect the organic components unirradiated by UV and prevent aging reaction. This part of the organic matter is the support that affects the connection of film particles, so the mechanical properties of the film remain at the level when it is not exposed to ultraviolet radiation. In addition, the main chemical bond in SiO_2 is Si-O-Si and the chemical property is stable. It is not easy to generate redox reaction under the action of ultraviolet light. Therefore, the hardness of the SiO_2 film is not changed when exposed to ultraviolet light. The reason why the adhesion has not declined is that the innermost layer of the film is bonded to the glass. Since the aging effect of ultraviolet rays has not reached the position where the film is bonded to the substrate, the adhesion has not decreased.

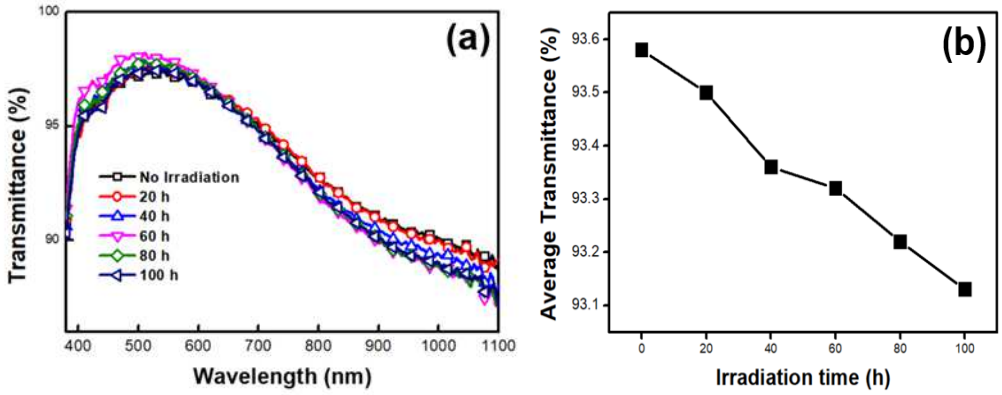


Fig. 8. (a) Transmission spectra of SiO_2 film after ultraviolet irradiation; (b) The influence of ultraviolet irradiation time on the average transmittance of 380-1100 nm wave band.

Figure 8 (a) shows the influence of the irradiation time of the ultraviolet lamp on the transmittance of the film with 6 ml IBTS addition. It can be seen that the spectral trend of the transmittance is similar and all curves decreased slightly at 800-1100 nm. Figure 8 (b) shows the influence of the time on the integrated transmittance at 380-1100 nm. It can be seen that with the increase of the irradiation time of ultraviolet light, the integrated transmittance of the film decreased with 0.45 percentage points. This may be due to the internal oxidation of the film caused by ultraviolet light, changing the molecular structure. The voids of the film were filled and the refractive index increased, which reduced the anti-reflection effect and the transmittance of the film.

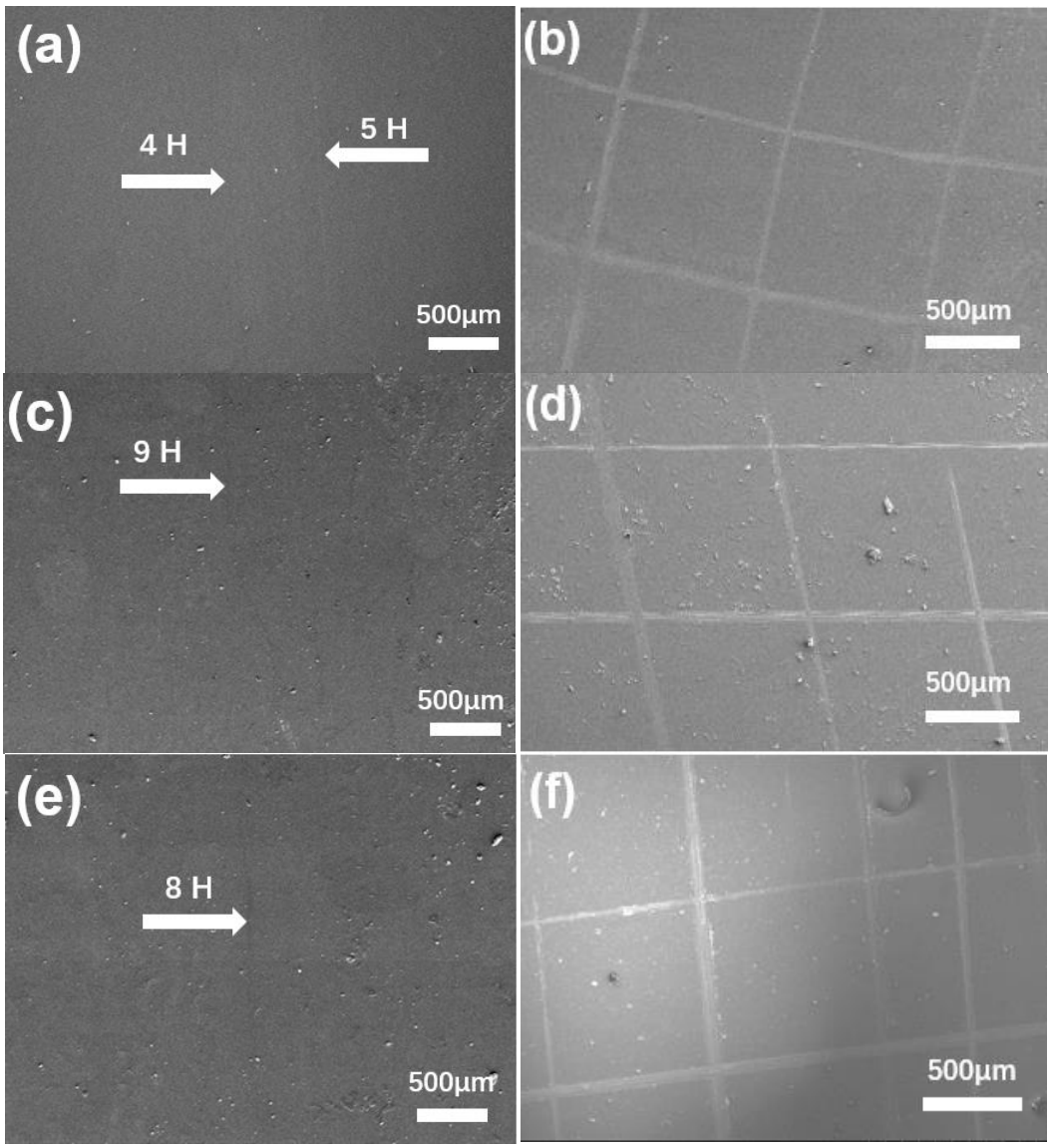


Fig. 9. Film surface morphology after hardness and adhesion test: (a) And (b) hardness scratch diagram and adhesion scratch diagram of film without IBTS after 60h immersion; (c) And (d) hardness scratch diagram and adhesion scratch diagram of film with 6 ml IBTS after 80h immersion; (e) And (f) hardness scratch diagram and adhesion scratch diagram of film with 6 ml IBTS after 100h immersion.

Shown in Fig. 9 are the SEM images of the film surface scratched with 9H pencil hardness tester and adhesion tester after immersing in 0.5mol/L hydrochloric acid solution. Fig. 9 (a) shows the SEM image of the film without IBTS after being soaked in hydrochloric acid solution for 80 h and then marked with pencil hardness. The hardness was 4 H. The soaking time of Figure (c) and (e) was 80 h and 100 h respectively, which showed that when the soaking time was 80 h, scratches begin to appear and he hardness of the film decreased(8H). Fig. 9 (b) shows the SEM image of the film without IBTS after being soaked in hydrochloric acid solution for 80 h and scratched with the adhesion tester. The adhesion is Grade 0. Shown in Figure (d) and (f) are the films soaking for 80 h and 100 h, respectively. When the film soaking time was 80 h, the grid began to peel off. When the immersion time was 100 h, the adhesion was still Grade 1. This is because the immersion of hydrochloric acid for the film

made the mPEG and other organic substances in the film gradually react with hydrochloric acid, which led to dehydration. Dehydration caused the loss of a large number of oxygen groups, which reduced the hydrogen bond content and mechanical properties.

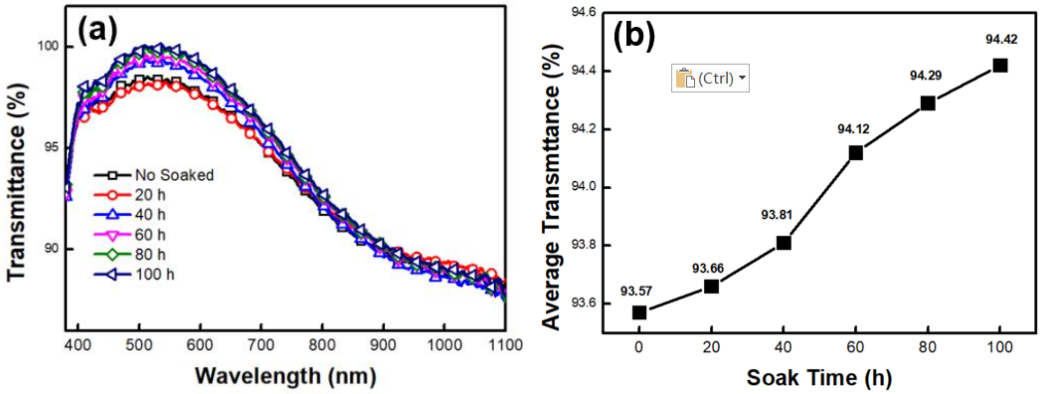


Fig. 10. (a) Effect of immersion time in hydrochloric acid solution on the light transmittance spectra of the film; (b) The effect of immersion time in hydrochloric acid solution on the average transmittance of the film at 380-100 nm.

Fig. 10 (a) is the curves of the light transmittance of the film with 6 ml of IBTS addition after immersion in hydrochloric acid solution. It can be found that the trend of the curves at 380-1100 nm waveband was similar. With the increasing of the film soaking time, the transmittance was improved a little. This is due to the existence of hydroxyl groups on the surface of SiO_2, and the defects on the surface of SiO_2 particles caused by the corrosion treatment of hydrochloric acid solution made the pores form between the original film particles. The improved porosity reduced the refractive index of the film [30].

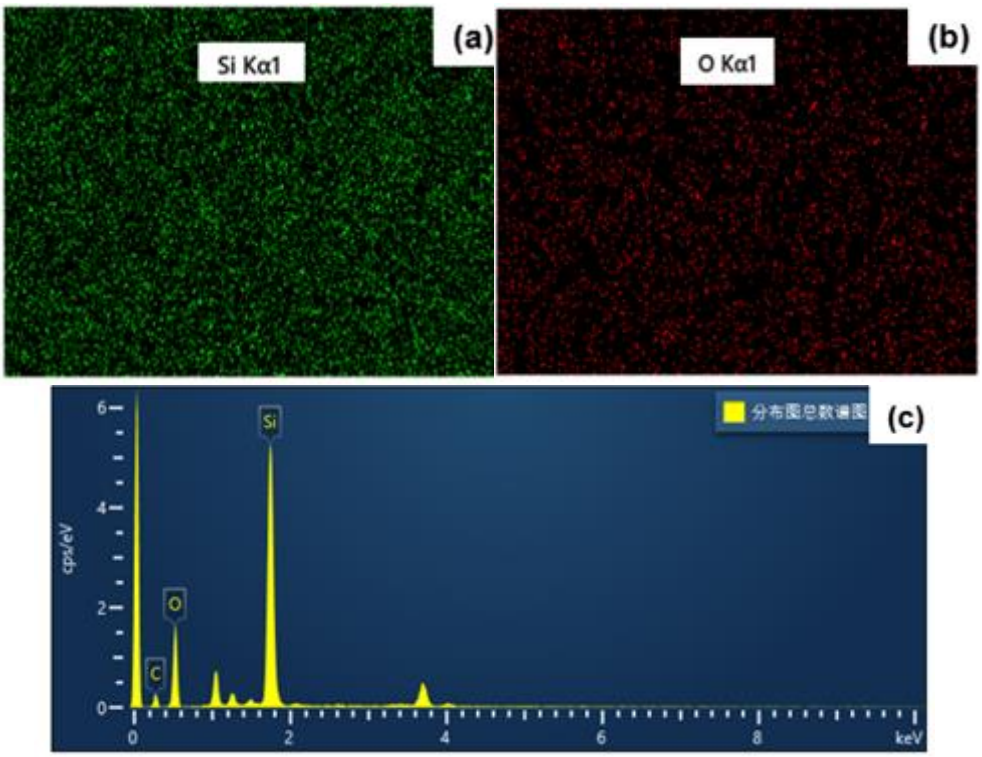


Fig.11. EDX map of the film with 6 ml of IBTS addition after soaking for 100h: (a)Si distribution; (b)Sb distribution; (c) Spectra for all elements.

Figure 11 shows the EDX map of the film with 6 ml of IBTS addition after soaking for 100 h. (a) and (b) are the distributions of Si and O and (c) is the element distribution of the film. Obviously, there is no Cl-ion in the spectra and it can be inferred that no chloride ion entered into the film after immersion in hydrochloric acid solution. This is because isobutyl blocked the channel in the pores, which also blocked the entry of harmful chloride ions carried in water molecules. Since the mechanical properties of the film without IBTS were reduced as indicated above, it can be considered that the internal of the film was reacted with hydrochloric acid.

4 Conclusion

In this paper, IBTS was used as blend, hydrolyzed with TEOS. Polyethylene glycol monomethyl ether was used as pore forming agent and acid catalyzed sol-gel method was used to prepare SiO_2 anti-reflection film with high reflectivity, high mechanical properties and good weather fastness on glass substrate. The influence of the amount of IBTS added on the morphology and properties of the film was studied. The weatherability of the film was also tested with UV lamp irradiation test and acid solution corrosion test. The results showed that the anti-reflection film prepared with IBTS had good anti-reflection performance. With the increase of the amount of IBTS added, the porosity of the film increased first and then decreased and the refractive index of the film decreased first and then

increased. When the amount of IBTS addition was 6 ml, the average transmissivity of the glass in the 380-1100 nm wavelength range increased by 4.4%. The adhesion of the film reached above grade 0 and the hardness reached above 9 H. Compared with the blank glass cover, the coated cover improved the efficiency of mono-crystalline silicon solar cells by 0.59%, reaching 12.26%. In the UV irradiation test, the mechanical properties of the film did not change significantly with the increase of the UV lamp irradiation time, but the optical properties decreased with 0.45 percentage points. In the acid solution immersion experiment, with the increase of the acid solution corrosion time, the hardness of the film decreased to 8H and the adhesion decreased to level 1. The optical performance slightly increased, with a maximum increase of 0.8%.

References

[1] Johnson C C , Wydeven T , Donohoe K . Plasma-enhanced CVD silicon nitride anti-reflection film for solar cells[J]. Solar Energy, 1983, 31(4):355-358.

[2] Su W T, Li B , Liu D Q , et al. Characterization and application of cerium fluoride film in infrared anti-reflection film[J]. Infrared Physics & Technology, 2009, 52(5):204-207.

[3] Huang J J , Lin C C , Wuu D S . anti-reflection and passivation property of titanium oxide thin film on silicon nanowire with liquid phase deposition[J]. Surface & Film Technology, 2017:S0257897217300269.

[4] Zhao C , Ma C , Liu J , et al. Preparation of wide optical spectra and high anti-reflection MgF2 thin film with SF6 as reactive gas[J]. Materials Research Express, 2020, 7(2).

[5] Ma C , Wang L , Fan X , et al. Broadband anti-reflection and hydrophobic CaF2 film prepared with magnetron sputtering[J]. Applied Surface Science, 2021, 560(6):149924.

[6] Cecilia A S , Maider M , Agnieszka T . Antireflective mesoporous silica film with optimization of water content in acid-catalyzed sol-gel method for application in glass covers of concentrated photovoltaic modules[J]. Journal of Colloid & Interface Science, 2018:S0021979718311184-.

[7] Wang Y , Nie L , Liu J . Preparation of hydrophobic SiO_2 film with high transmittance with sol mixing method[J]. Chemical Physics Letters, 2020, 747:137331.

[8] Yuan Y , Yan G H , Huang S H , et al. Preparation of hydrophobic SiO_2/PMHS sol and ORMOSIL antireflective film for solar glass cover[J]. Solar Energy, 2016, 130(Jun.):1-9.

[9] Chi F , Zeng Y , Liu C . Tuning refractive indices of sol-gel silica film with ammonia treatment for broadband anti-reflection applications[J]. Optik - International Journal for Light and Electron Optics, 2020, 224:165501.

[10] Nagel H, Metz A, Hezel R, Porous SiO_2 film prepared with remote plasma-enhanced chemical vapour deposition - a novel anti-reflection film technology for photovoltaic modules[J]. SOLAR ENERGY MATERIALS AND SOLAR CELLS, 2001.

[11] Enhancing performance of perovskite solar cells with efficiency exceeding 21% via a graded-index mesoporous aluminum oxide anti-reflection film[J]. Nanotechnology, 2020, 31(27):275407 (7pp).

[12] Hai, Liu, Lijie, et al. Ultraviolet light aging properties of PVC/CaCO3 composites[J]. Journal of Applied Polymer Science, 2013.

[13] B, B, Troitskii, et al. Preparation of anti-reflection film from silicon dioxide on glass and quartz with the sol-gel method with oligoethers[J]. Glass Physics & Chemistry, 2010.

[14] Yu J , Li S , Hou D , et al. Hydrophobic silane film film for the inhibition of water ingress into the nanometer pore of calcium silicate hydrate gels[J]. Physical Chemistry Chemical Physics, 2019, 21.pccp,13.14.

[15] Nan D U , Wang S X , Zhao Q , et al. Effects of boric acid on microstructure and corrosion resistance of boric/sulfuric acid anodic film on 7050 aluminum alloy[J]. Transactions of Nonferrous Metals Society of China, 2012, 22(7):1655-1660.
[16] Li XK， Liu X， Study on Corrosion Resistance of Superhydrophobic Film Prepared on the Surface of 2024 Aluminum Alloy[J] INTERNATIONAL JOURNAL OF ELECTROCHEMICAL SCIENCE,2022,17(2)
[17]C García-Cabezón, Salvo-Comino C , C García-Hernández, et al. Nanocomposites of conductive polymers and nanoparticles deposited on porous material as a strategy to improve its corrosion resistance[J]. Surface and Film Technology, 2020, 403(6).
[18] Li S , Zhang W , Liu J , et al. Protective Mechanism of Silane on Concrete upon Marine Exposure[J]. Film, 2019, 9(9):558.
[19] Yg A , Pz A , Sl A , et al. Superior corrosion resistance of mild steel coated with graphene oxide modified silane film in chlorinated simulated concrete solution.
[20] General preparation of paint film. 1992; GB/T 1727-1992.
[21] Paints and varnishes—Cross cut test for film. 1998; GB/T 9826—1998.
[22] Ygab C , Jlab C , Bdab C . Improvement of the dust removal performance of a high-transmittance SnO_2–SiO_2 film with Sb doping - ScienceDirect[J]. Ceramics International, 2020.
[23] Zhang G , Xu Y , Xu D , et al. Pressure-induced crystallization of amorphous SiO_2 with silicon-hydroxy group and the quick synthesis of coesite under lower temperature[J]. High Pressure Research, 2008, 28(4):641-650.
[24] Stefano V C , Riccardo T , D Alessandro, et al. Thermal Behavior and Structural Study of SiO_2/Poly(ε-caprolactone) Hybrids Synthesized via Sol-Gel Method[J]. Materials, 2018, 11(2):275.
[25] KIRSZENSZTEJN P, KAWALKO A, TOLINSKA A, et al. Synthesis of SiO2–SnO2 gels in water free conditions[J]. Journal of Porous Materials, 2010,18(2): 241-249.
[26] CANEVARI T C, ARGUELLO J, FRANCISCO M S P, et al. Cobaltphthalocyanine prepared in situ on a sol–gel derived SiO2/SnO2 mixed oxide: Application in electrocatalytic oxidation of oxalic acid[J]. Journal of Electroanalytical Chemistry, 2007, 609(2): 61-67.
[27] PARLER C M, RITTER J A, AMIRIDIS M D. Infrared spectroscopic study of sol-gel derived mixed-metal oxides[J]. Journal of Non-Crystalline Solids,2001, 279(2-3): 119-125.
[28] CARDOSO W. Synthesis and acidic properties of the SiO2/SnO2 mixed oxide sobtained with the sol–gel process. Evaluation of immobilized copper hexacyanoferrate as an electrochemical probe[J]. Solid State Ionics, 2004, 167(1-2): 165-173.
[29] He H, Li H , Zhang Y , et al. Enhanced high reflectance SiO2-Ag-SiO2 thin film adhesion for Concentrating Solar Power reflector[J]. Surfaces and Interfaces, 2017, 8:225-229.
[30] Zhang S, Zhao X , Wang P , et al. Preparation of superhydrophilic silicate film with sol–gel for double-wavelength broadband antireflective film[J]. Journal of Sol-Gel Science and Technology, 2019, 92(14):1-9.